Letter

Creasing of flexible membranes at vanishing tension

Weria Pezeshkian [1] and John H. Ipsen [2,*]

[1]*Groningen Biomolecular Sciences and Biotechnology Institute and Zernike Institute for Advanced Materials, University of Groningen, Groningen, Netherlands*

[2]*MEMPHYS/PhyLife, Department of Physics, Chemistry and Pharmacy (FKF), University of Southern Denmark, Campusvej 55, 5230 Odense M, Denmark*

(Received 2 November 2020; accepted 30 March 2021; published 16 April 2021)

The properties of freestanding tensionless interfaces and membranes at low bending rigidity κ are dominated by strong fluctuations and self-avoidance and are thus outside the range of standard perturbative analysis. We analyze this regime by a simple discretized, self-avoiding membrane model on a frame subject to periodic boundary conditions by use of Monte Carlo simulation and dynamically triangulated surface techniques. We find that at low bending rigidities, the membrane properties fall into three regimes: Below the collapse transition κ_{BP} it is subject to branched polymer instability where the framed surface is not defined, in a range below a threshold rigidity κ_c the conformational correlation function are characterized by power-law behavior with a continuously varying exponent α, $2 < \alpha \leqslant 4$ and above κ_c, $\alpha = 4$ characteristic for linearized bending excitations. Response functions specific heat and area compressibility display pronounced peaks close to κ_c. The results may be important for the description of soft interface systems, such as microemulsions and membranes with in-plane cooperative phenomena.

DOI: 10.1103/PhysRevE.103.L041001

I. INTRODUCTION

Since the 1960s it has been understood that the properties of low-tension liquid interfaces serve as the basis for a wealth of phenomena in nature, including detergent effect, microemulsions, and biological membranes. Despite the longstanding investigations of such interfaces, basic questions remain unanswered. Here, we will address the physical properties of tensionless, hyperflexible fluid interfaces. In 1983 it was established that freestanding, flexible, fluid, self-avoiding surfaces cease to exist as smooth 2D manifolds due to an entropy-driven collapse into branched polymerlike configurations [1]. Possible ways to deal with this problem are to stabilize the surface by a frame, by applying tension, constrain a fixed volume within a closed surface, or to provide some internal stiffness to the surface. The simplest correction to the capillary free energy for interfaces is the mean curvature elasticity introduced in 1973 by Wolfgang Helfrich for the description of membrane shape problems [2]:

$$\mathcal{H} = \mu_0 A + \frac{\kappa}{2}\int dA(2H)^2. \tag{1}$$

Here, A is the surface area with the conjugated internal tension μ_0 and H is the local mean curvature with the associated elastic constant κ, the bending rigidity. The form Eq. (1) is fixed by numerous symmetries, including surface reparametrization invariance and Euclidean symmetry of space. If the surface can perform topological transformations or have boundaries, then there will furthermore be a Gaussian curvature contribution, which will not be relevant for our considerations. Besides these contributions to the energy, the surface is subject to self-avoidance. Equation (1) is well suited for the description of freestanding lipid bilayer membranes, which can be considered as incompressible and semiflexible with $\kappa \sim 10\,k_BT$ and μ_0 small. However, the effective bending rigidity can be dramatically reduced $\kappa \simeq k_BT$, e.g., for membranes with in-plane lipid phase transitions [3,4], lipid mixtures with surfactantlike components [5], membranes with I/O symmetry breaking inclusions [6–8], membranes containing triglycerides [9], or even membranes with rigid trans-membrane inclusions [10]. Conformational fluctuations at low κ can cause new surface phenomena, e.g., unbinding of multilayers [11] or a new mechanism of aggregation of soft membrane embedded inclusions [8], supplementing depletion effect [12,13], and thermal Casimir effect [14,15] of rigid inclusions. The most powerful numerical method for characterizing low κ properties of self-avoiding surfaces is the dynamic triangulated surface technique (DTS). Early studies of self-avoiding vesicles by DTS with discretized Eq. (1) displayed a discontinuous inflation-deflation transition at finite-pressure difference Δp at $\kappa = 0$ [16] and for $\Delta p = 0$ a cusp was found in the specific heat in the range $\kappa \sim 1 - 3\,k_BT$ [17]. It has been tempting to associate this anomaly with the continuous crumpling transitions observed for self-intersecting (phantom) DTS models [18,19] and tethered membrane (fixed triangulation) models [20]. However, when self-avoidance is introduced for tethered membranes the crumpling transition is abolished [21].

The analysis of the thermal properties of this surface involves the calculation of the partition function,

$$Z(\mu_0, \kappa, A) = \int d[\vec{X}]\exp(-\beta\mathcal{H}), \tag{2}$$

*ipsen@memphys.sdu.dk

which is a very complicated object to handle, even with computer simulation techniques. A tool for doing practical calculations is to frame the membrane, i.e., limit the analysis to a patch of the surface fluctuating around a planar frame of area A_p. The position of the membrane is here given as $\vec{X} = [\vec{x}, z(\vec{x})]$, where $\vec{x} = (x_1, x_2)$, the so-called Monge representation (or gauge). The calculations thus become more tractable, e.g., the total area becomes

$$A[z(\vec{x})] = \int_{A_p} d^2\vec{x}\sqrt{1 + [\vec{\nabla} z(\vec{x})]^2}. \tag{3}$$

An important result obtained from such calculations for semiflexible membranes is that the bending rigidity renormalizes to zero at some persistence length $\xi \simeq l_0 \exp\left(\frac{4\pi\kappa}{3k_BT}\right)$, where the surface normals become uncorrelated [22], while the surface appears smooth on shorter length scales. Thus, in the thermodynamic limit unconstrained fluid membranes are expected to be *crumpled*, i.e., branched polymerlike on length scales larger than ξ. This picture has been confirmed for self-avoiding vesicles by computer simulation techniques where the, e.g., vesicle volume is found to display a smooth cross-over from semiflexible behavior at vesicle sized below ξ to branched polymerlike scaling above ξ [23–25]. But typically ξ is much larger than both l_0, a microscopic length scale of order bilayer thickness, and the linear extension of the physical membranes. However, it remains unclear to which extent the rigid membrane analysis can be extended to low κ with some corrections to ξ [24] or if new physical phenomena will emerge in this regime for self-avoiding surfaces [26]. A recent numerical analysis of the thermodynamics of a framed, semiflexible membrane at fixed A showed that even such surfaces cease to exist for membranes below a threshold bending rigidity $\kappa_{\mathrm{BP}} \sim k_BT$ at vanishing tension [27]. We have in this work analyzed response functions and the two-point correlation function $\langle z(\vec{x})z(\vec{x}')\rangle$ in the regime $\kappa \geqslant \kappa_{\mathrm{BP}}$ for framed, tensionless self-avoiding surfaces.

To help interpreting the simulation data we first conduct some considerations about the limitations in the behavior of the correlation function $\langle z(\vec{x})z(\vec{x}')\rangle$. Framing a fluid surface model has some consequences, which was recognized already in the context of drumhead models [28] and restated for membranes [29,30]. The frame gives rise to a new thermodynamic variable, the projected area A_P, and thus a conjugated frame tension τ (or physical tension). Furthermore, the Euclidean invariance has been broken by the frame which is reflected as constraints on the correlation functions. The relevant partition function becomes

$$\begin{aligned} &Z(A_p, A, \mu_0, h(\vec{x})) \\ &\quad = \int D[z(\vec{x})]\delta\{A \\ &\qquad \times [z(\vec{x})] - A\}\left[-\beta\left(\mathcal{H} - \int_{A_p} d^2\vec{x}h(\vec{x})z(\vec{x})\right)\right], \end{aligned} \tag{4}$$

with the associated free energy $F[A_p, A, h(\vec{x})] = -k_BT \ln\{Z[A_p, A, h(\vec{x})]\}$. The external field $h(\vec{x})$ is introduced to generate mean conformations and correlation functions, e.g., $\langle z(\vec{x})\rangle_{h(\vec{x})} = \bar{z}(\vec{x}) = -\frac{\delta F(A_p, A, h(\vec{x}))}{\delta h(\vec{x})}$. For $h(\vec{x}) = 0$ a membrane patch is fluctuating around the plane of the frame we expect $\bar{z}(\vec{x}) = 0$ and the $2D$ translational invariance imposed that the two-point correlation function takes the form

$$\begin{aligned} g(\vec{x} - \vec{y}) &= \langle [z(\vec{x}) - \bar{z}(\vec{x})][z(\vec{y}) - \bar{z}(\vec{y})]\rangle_{h=0} \\ &= -k_BT\left(\frac{\delta^2 F}{\delta h(\vec{x})\delta h(\vec{y})}\right)_{h=0}. \end{aligned} \tag{5}$$

Furthermore, the physical frame tension can be obtained from the thermodynamic equation of state $\tau = \left(\frac{\delta F[A_p, A, h(\vec{x})]}{\delta A_p}\right)_{h=0}$. From Legendre transformation the free energy $\Gamma[A_p, A, \bar{z}(\vec{x})] = F[A_p, A, h(\vec{x})] + \int_{A_p} d^2\vec{x}h(\vec{x})\bar{z}(\vec{x})$ can be constructed which contains the same thermodynamic information as F. The equilibrium $\bar{z}(\vec{x})$ at $h = 0$ is obtained from the minimum of Γ where $\Gamma^{(2)}(\vec{x}, \vec{y}) = \frac{\delta^2\Gamma[A_p, \bar{z}(\vec{x})]}{\delta\bar{z}(\vec{y})\delta\bar{z}(\vec{z})}$ is positive definite. $\Gamma^{(2)}$ is related to the correlation function g, e.g., their Fourier transform obey $g(\vec{k})\Gamma^{(2)}(\vec{k}) = k_BT$. Both $\bar{z}(\vec{x})$ and A_p are sensitive to rotation of the frame while Γ is not, which gives rise to a strong constraint (Ward identity) on the form of the leading terms

$$\Gamma[A_p, A, \bar{z}(\vec{x})] = \tau\int_{A_p} d^2\vec{x}\sqrt{1 + (\vec{\nabla}\bar{z})^2} + \cdots \tag{6}$$

Equation (6) strongly resembles the first term of Eq. (1) with application of Eq. (3). However, there are important differences. While $z(\vec{x})$ in Eq. (3) represents the instantaneous configuration of the surface then $\bar{z}(\vec{x})$ is a mean configuration of the surface under the influence of the field $h(\vec{x})$. Furthermore, the prefactor of Eq. (6) is the physical frame tension, and not the internal tension of Eq. (1). The undefined terms in Eq. (6) are contributions to Γ which are insensitive to the Euclidean symmetry (regular or singular terms involving higher order derivatives of $\bar{z}$). It is thus clear that for small-$\vec{k}$ we have $\Gamma^{(2)}(\vec{k}) = \tau\vec{k}^2 + \cdots$ for $\tau \neq 0$ and $\Gamma^{(2)}(\vec{k}) \sim |\vec{k}|^\alpha$ with $\alpha \geqslant 2$ in general. In the tension less case all the k^2 terms vanishes and such contributions induced by fluctuations will cancel due to the Euclidean symmetry of Eq. (1) and thus $\alpha > 2$. In the rigid limit at large κ we expect $\alpha = 4$, from simple linearization of the curvature elasticity in Eq. (1). The corrections to order $\frac{k_BT}{\kappa}$ will give rise to the well-known renormalization of the bending rigidity [22], but $\alpha = 4$ remains as the leading power. In this work we are interested in the opposite limit with small bending rigidities, where very few results are known. From the above considerations it is clear that $2 < \alpha \leqslant 4$ for $\tau = 0$ and κ small. In the simulations presented below τ is a controllable parameter, while the leading power α can be obtained from analysis of configurational fluctuation.

II. METHOD

The method used here follows closely the setup used in Ref. [8]. The fluid membrane is modeled by a dynamically triangulated, self-avoiding surface subject to periodic boundary conditions in a rectangular frame characterized by N_v vertices, N_t triangles, and N_l links fixed by the relation $6N_v = 3N_t = 2N_l$. The self-avoidance is enforced by a spherical bead of diameter d at each vertex and a maximum tether length between neighboring vertices $\sqrt{3}d$. This method involves a set of discretized geometrical operations to calculate vertex-based quantities, like the surface area $A(\nu)$ and the descrete

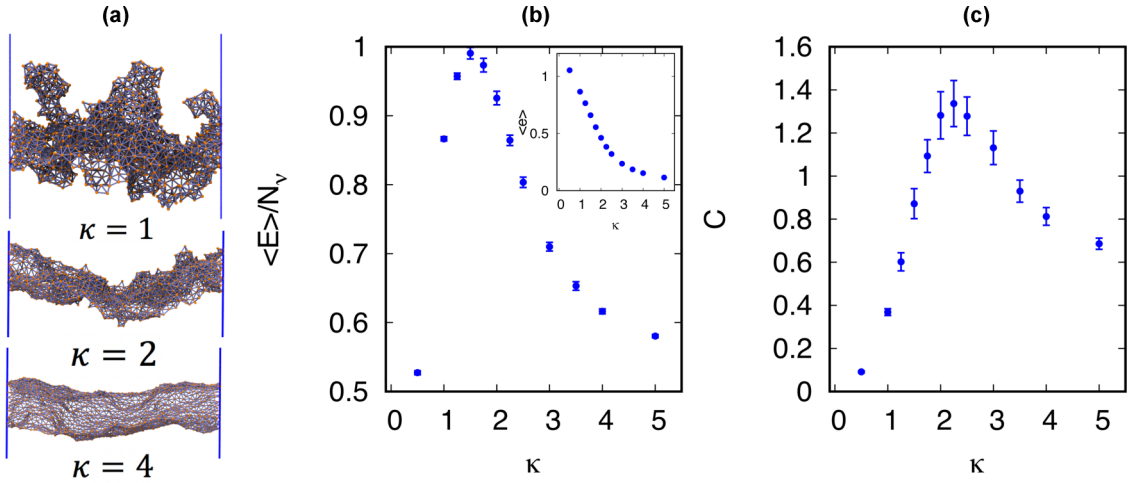

FIG. 1. (a) Snapshots of membranes with different bending rigidity κ. (b) $\langle E\rangle/N_v$ versus κ. In the inset $\langle e\rangle = \langle E\rangle/(\kappa N_v)$ is shown. (c) The specific heat $C = (\langle E^2\rangle - \langle E\rangle^2)/N_v$ versus κ. In all systems, the number of the vertices is $N_v = 1840$ and the systems were simulated at zero tension ($\tau = 0$).

shape operator $S(\nu)$ described in detail in Ref. [31]. $S(\nu)$ is constructed from the directional curvatures for the piecewise triangular surface defined so that it together with the induced Euclidean metric make a consistent discrete surface differential geometry which comply with the continuum surface differential geometry as the mesh-size becomes small. The local principal frame of reference (Darboux frame) for $S(\nu)$ is given by the normal vector $\mathbf{N}_\nu$ and the principal curvature vectors $\mathbf{X}_1(\nu), \mathbf{X}_2(\nu)$ with associated local principal curvatures $c_1(\nu), c_2(\nu)$ as eigenvalues. The discretized Helfrich mean-curvature elastic energy Eq. (1) thus becomes

$$E = \frac{\kappa}{2}\sum_{\nu}^{N_v} A(\nu)[c_1(\nu) + c_2(\nu)]^2. \tag{7}$$

The equilibrium properties of simple vesicles based on this discretization procedure have been analyzed by Monte Carlo simulation and shown consistent with previous methods [31]. In addition to the two standard Monte Carlo moves for DTS, link flip and vertex moves, framed membranes require an additional move to control the membrane frame area A_p at constant τ[8]. The numerical estimate of $\langle z(\vec{k})z(-\vec{k})\rangle$ is obtained by 2D Fourier transform $z(\vec{k})$ of $z(\vec{x}_i)$ for single snapshots and $z(\vec{k})z(\vec{k})^*$ are averaged over the snapshots. Furthermore, we analyze the thermal response functions at $\tau = 0$: The heat capacity $C = \frac{1}{N_v}(\langle E^2\rangle - \langle E\rangle^2)$ and the projected area compressibility $K = \frac{1}{\langle A_p\rangle}(\langle A_p^2\rangle - \langle A_p\rangle^2)$.

III. RESULTS AND DISCUSSION

The Monte Carlo simulations of the triangulated surface model were performed with fixed κ, N_v, and τ. Without loss of generality we set $k_BT = 1$ and $d = 1$ throughout the analysis. The simulations are performed with $N_v = 1840$ and $\tau = 0$, while κ was varied from 0 to 5. At each system condition simulations of 10^7 MCS was performed for 24 replicas with varying start configurations. For decreasing κ the membrane appears increasingly rough as shown in Fig. 1(a). At $\kappa = 4$ the surface appears locally smooth as expected for rigid membranes, at $\kappa = 2$ short length scale roughness prevails while local protrusions dominate at $\kappa = 1$. The specific heat C has been an indicator of membrane crumpling in computer simulations of vesicles. The framed membrane C displays a single cusp at $\kappa_c \simeq 2$ [Fig. 1(c)], which is in good agreement with the results found from DTS simulations of fluid vesicles [17,31]. This cusp is accompanied with a local roughening of the membrane as indicated in Fig. 1(a). The average energy $\langle E\rangle/N_v$ shows an approximative quadratic dependence of κ with a maximum below κ_c [Fig. 1(b)]. This behavior is illuminated in the inset of Fig. 1(b) where a fit is parametrized as $\langle e\rangle = \langle E\rangle/(\kappa N_v) \simeq 1.06 - 0.40(\kappa - \kappa_{\rm BP})$ in the range $\kappa_{\rm BP} < \kappa < \kappa_c$. $\kappa_{\rm BP} = 0.5 \pm 0.1$ mark the discontinuous collapse of the membrane, where even the local surface characteristics disappears and the branched polymerlike configurations with cutoff-sized branch thickness prevails for $\kappa < \kappa_{\rm BP}$. $\langle A_p\rangle$ is generally increasing for $\kappa > \kappa_{\rm BP}$ as shown in Fig. 2(a) starting at $\langle A_p\rangle/N \simeq 0.5$ for $\kappa = \kappa_{\rm BP}$. The obtained $\langle A_p\rangle$ is in overall agreement with the thermodynamic analysis in Ref. [27]. For for $\kappa > 3$ $\langle A_p\rangle$ varies weakly as expected for locally smooth surface configurations [Fig. 1(a)]. The transition at κ_c can also be observed in the lateral compressibility K_P [Fig. 2(b)] as a distinct peak indicating a dramatic lateral softening of the membrane. The peaks in C or K_P are very weakly dependent of the system size (not shown) as previously seen in simulations of fluid vesicles [17]. It is thus interesting to explore the structural changes associated with the transition at κ_c, e.g., by characterization of $\langle z(\vec{k})z(-\vec{k})\rangle$. Short-distance overhangs at the smallest κ [see Fig. 1(a)] may cause the numerically obtained $\langle z(\vec{k})z(-\vec{k})\rangle$ to be ill-defined at high k, while it is well-determined at low k which is the focus of interest. In Fig. 2(d) is shown the fit of $\langle z(\vec{k})z(-\vec{k})\rangle$ versus low k for a range of κ values. The simulation results show that $\langle z(\vec{k})z(-\vec{k})\rangle \propto |\vec{k}|^{-\alpha(\kappa)}$, where the exponent $\alpha(\kappa)$ is plotted versus κ in Fig. 2(c). $\alpha(\kappa) \simeq 4$ for $\kappa > \kappa_c$ as expected from linearization of the Helfrich bending elastic energy Eq. (1). The estimated effective bending rigidity is slightly reduced

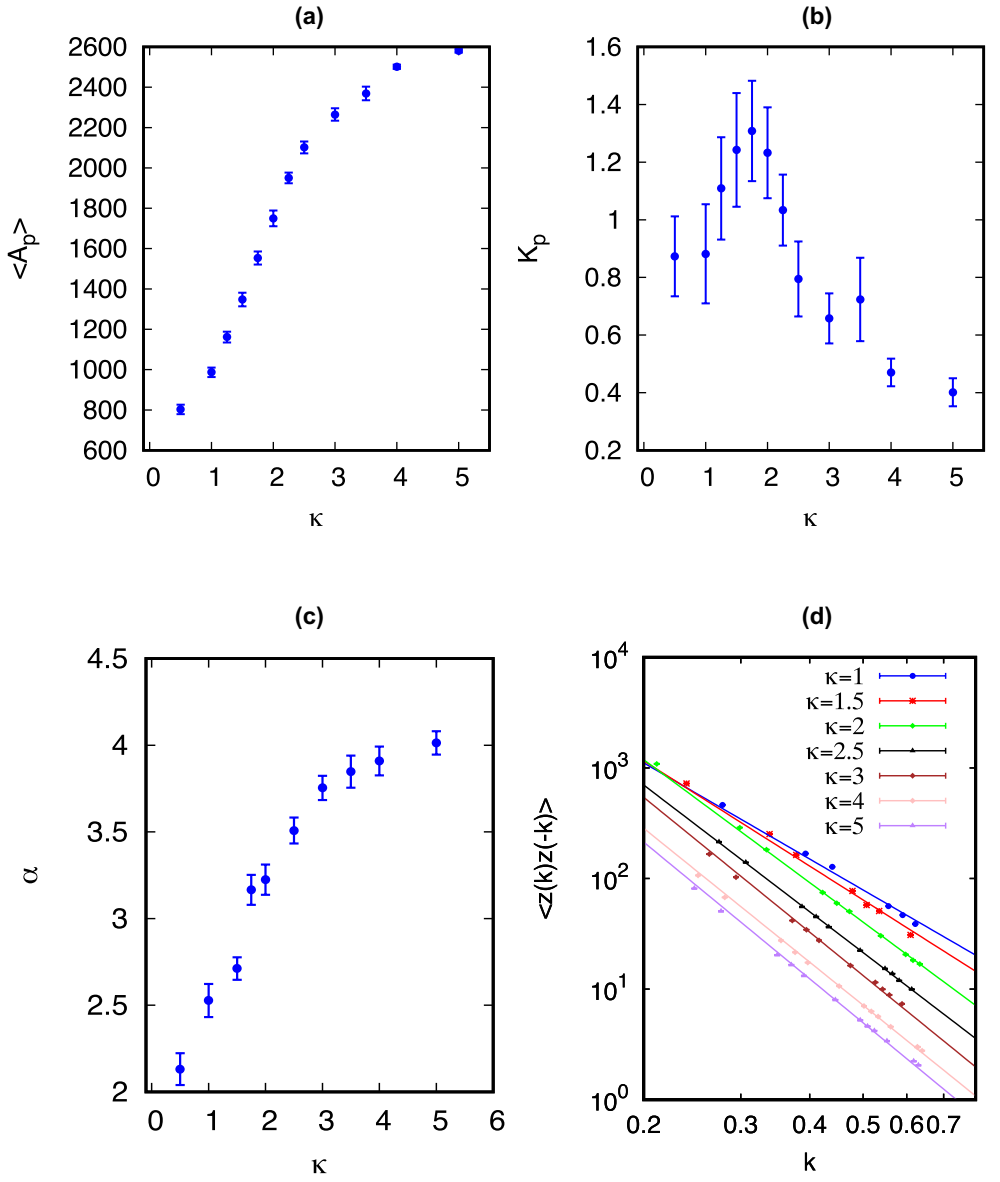

FIG. 2. (a) $\langle A_p \rangle$ versus κ. (b) Projected area compressibility $K_p = (\langle A_p^2 \rangle - \langle A_p \rangle^2)/\langle A_p \rangle$ versus κ. (c) The correlation function is found to obey $\langle |z(\vec{k})|^2 \rangle \propto |\vec{k}|^{-\alpha(\kappa)}$, where $\alpha(\kappa)$ is plotted versus κ. For $\kappa > \kappa_c$ $\alpha(\kappa) \simeq 4$, while $\alpha(\kappa)$ is nearly linear in κ in the range $\kappa_{\rm BP} < \kappa < 3$. (d) Data for $\langle |z(\vec{k})|^2 \rangle$ at low k. The error bars are smaller than the symbols for the data points. The lines indicate the fit to the above power law.

compared to the bare κ in this regime [8]. For $\kappa_{\rm BP} < \kappa < \kappa_c \alpha(\kappa)$ vary with κ in an approximately linear fashion with $\alpha(\kappa_{\rm BP}) \simeq 2$ and $\alpha(\kappa) \simeq 4$ for $\kappa < \kappa_c$.

Continuously varying power-law exponents are common in 2D physics due to Wagner-Mermin theorem [32] for systems with Abelian continuous symmetry. In the context of a single membrane it has been proposed that a crystalline, phantom membrane have a continuously varying Hausdorff dimension [33] and a hexatic membrane has a *crinkled* phase with continuously varying exponent for the conformational correlation function [26]. While these examples represent low-temperature properties of surfaces with in-plane stiffness, the presented behavior of a fluid membrane with self-avoidance are found in the opposite limit (high-temperature conditions). A more relevant candidate theory is the *bumpy* phase proposed by David and Guitter [34] based on large-d analysis of Helfrich's model, which is characterized by curvature inhomogeneities at ξ length-scale at low κ. However, a theoretical prediction for the $g(\vec{k})$ beyond the mean-field theory for surfaces in $d = 3$ is not available. Finally, an analogy may be found in the rough phase of SOS-models [35] where the roughening is associated with a Kosterlitz-Thouless–like transition. These models lack self-avoidance or only permit highly restricted configurations and may thus not be applicable to this study where both self-avoidance and wild configurations are found to be important at low κ. We therefore conclude that our DTS simulations of a framed, fluid, and self-avoiding membrane have revealed a new rough surface regime at low κ and vanishing tension which is dominated by extensive configurational fluctuations characterized by a power-law configurational correlation function with a continuously varying power.

[1] B. Durhuus, J. Fröhlich, and T. Jonsson, Self-avoiding and planar random surfaces on the lattice, Nucl. Phys. B **225**, 185 (1983).

[2] W. Helfrich, Elastic properties of lipid bilayers: Theory and possible experiments, Z. Naturforsch. C **28**, 693 (1973).

[3] T. Hønger, K. Mortensen, J. H. Ipsen, J. Lemmich, R. Bauer, and O. G. Mouritsen, Anomalous Swelling of Multilamellar Lipid Bilayers in the Transition Region by Renormalization of Curvature Elasticity, Phys. Rev. Lett. **72**, 3911 (1994).

[4] P. L. Hansen, L. Miao, and J. H. Ipsen, Fluid lipid bilayers: Intermonolayer coupling and its thermodynamic manifestations, Phys. Rev. E **58**, 2311 (1998).

[5] J. R. Henriksen, T. L. Andresen, L. N. Feldborg, L. Duelund, and J. H. Ipsen, Understanding detergent effects on lipid membranes: A model study of lysolipids, Biophys. J. **98**, 2199 (2010).

[6] H. P. Duwe, J. Kaes, and E. Sackmann, Bending elastic moduli of lipid bilayers: Modulation by solutes, J. Phys. **51**, 945 (1990).

[7] H. Bouvrais, P. Méléard, T. Pott, K. J. Jensen, J. Brask, and J. H. Ipsen, Softening of POPC membranes by magainin, Biophys. Chem. **137**, 7 (2008).

[8] W. Pezeshkian and J. H. Ipsen, Fluctuations and conformational stability of a membrane patch with curvature inducing inclusions, Soft Matter **15**, 9974 (2019).

[9] K. I. Pakkanen, L. Duelund, K. Qvortrup, J. S. Pedersen, and J. H. Ipsen, Mechanics and dynamics of triglyceride-phospholipid model membranes: Implications for cellular properties and function, Biochimica Biophysica Acta **1808**, 1947 (2011).

[10] M. Fošnarič, A. Iglič, and S. May, Influence of rigid inclusions on the bending elasticity of a lipid membrane, Phys. Rev. E **74**, 051503 (2006).

[11] J. Lemmich, K. Mortensen, J. H. Ipsen, T. Hønger, R. Bauer, and O. G. Mouritsen, Pseudocritical Behavior and Unbinding of Phospholipid Bilayers, Phys. Rev. Lett. **75**, 3958 (1995).

[12] S. Marčelja, Lipid-mediated protein interaction in membranes, Biochimica Biophysica Acta **455**, 1 (1976).

[13] K. Bohinc, V. Kralj-Iglič, and S. May, Interaction between two cylindrical inclusions in a symmetric lipid bilayer, J. Chem. Phys. **119**, 7435 (2003).

[14] M. Goulian, R. Bruinsma, and P. Pincus, Long-range forces in heterogeneous fluid membranes, Europhys. Lett. **22**, 145 (1993).

[15] W. Pezeshkian, H. Gao, S. Arumugam, U. Becken, P. Bassereau, J.-C. Florent, J. H. Ipsen, L. Johannes, and J. C. Shillcock, Mechanism of Shiga toxin clustering on membranes, ACS Nano **11**, 314 (2017).

[16] G. Gompper and D. M. Kroll, Inflated vesicles: A new phase of fluid membranes, Europhys. Lett. **19**, 581 (1992).

[17] D. M. Kroll and G. Gompper, The conformation of fluid membranes: Monte Carlo simulations, Science **255**, 968 (1992).

[18] S. M. Catterall, Extrinsic curvature in dynamically triangulated random surface models, Phys. Lett. B **220**, 207 (1989).

[19] R. L. Renken and J. B. Kogut, The crumpling transition in the presence of quantum gravity, Nucl. Phys. B **354**, 328 (1991).

[20] Y. Kantor and D. R. Nelson, Crumpling Transition in Polymerized Membranes, Phys. Rev. Lett. **58**, 2774 (1987).

[21] M. Plischke and D. Boal, Absence of a crumpling transition in strongly self-avoiding tethered membranes, Phys. Rev. A **38**, 4943 (1988).

[22] L. Peliti and S. Leibler, Effects of Thermal Fluctuations on Systems with Small Surface Tension, Phys. Rev. Lett. **54**, 1690 (1985).

[23] G. Gompper and D. M. Kroll, Phase diagram and scaling behavior of fluid vesicles, Phys. Rev. E **51**, 514 (1995).

[24] J. H. Ipsen and C. Jeppesen, The persistence length in a random surface model, J. Phys. I **5**, 1563 (1995).

[25] G. Gompper and D. M. Kroll, Random surface discretizations and the renormalization of the bending rigidity, J. Phys. I **6**, 1305 (1996).

[26] F. David, E. Guitter, and L. Peliti, Critical properties of fluid membranes with hexatic order, J. Phys. **48**, 2059 (1987).

[27] D. Hamkens, C. Jeppesen, and J. H. Ipsen, The tension of framed membranes from computer simulations, Eur. Phys. J. E **41**, 42 (2018).

[28] D. J. Wallace and R. K. P. Zia, Euclidean Group as a Dynamical Symmetry of Surface Fluctuations: The Planar Interface and Critical Behavior, Phys. Rev. Lett. **43**, 808 (1979).

[29] W. Cai, T. C. Lubensky, P. Nelson, and T. Powers, Measure factors, tension, and correlations of fluid membranes, J. Phys. II **4**, 931 (1994).

[30] O. Farago, Mechanical surface tension governs membrane thermal fluctuations, Phys. Rev. E **84**, 051914 (2011).

[31] N. Ramakrishnan, P. B. Sunil Kumar, and J. H. Ipsen, Monte Carlo simulations of fluid vesicles with in-plane orientational ordering, Phys. Rev. E **81**, 041922 (2010).

[32] N. David Mermin and H. Wagner, Absence of Ferromagnetism or Antiferromagnetism in One- or Two-Dimensional Isotropic Heisenberg Models, Phys. Rev. Lett. **17**, 1133 (1966).

[33] J. Ambjørn, B. Durhuus, and T. Jonsson, Kinematical numerical study of the crumpling transition in crystalline surfaces, Nucl. Phys. B **316**, 526 (1989).

[34] F. David and E. Guitter, Instabilities in membrane models, Europhys. Lett. **3**, 1169 (1987).

[35] D. B. Abraham, *Surface Structures and Phase Transitions—Exact Results in Phases, Transitions, and Critical Phenomena*, edited by C. Domb and J. L. Lebowitz (Academic Press, San Diego, CA, 1986), Vol. 10.